Research Article

NANOMATERIALS AND NANOTECHNOLOGY

Nanomaterials and Nanotechnology
Volume 7: 1–7
© The Author(s) 2017
DOI: 10.1177/1847980417702794
journals.sagepub.com/home/nax
SAGE

Green synthesis of graphene nanosheets and their in vitro cytotoxicity against human prostate cancer (DU 145) cell lines

Xin Zhu[1], Xiaolin Xu[1], Feng Liu[1], Jizhong Jin[1], Lintao Liu[1], Yi Zhi[2], Zhi-wen Chen[2], Zhan-song Zhou[2], and Jianjun Yu[1]

Abstract

A simple and green approach for the synthesis of polyphenol-functionalized reduced graphene oxide nanosheets is demonstrated, using leaf extract of *Citrullus colocynthis* as a deoxygenating agent. The *C. colocynthis* polyphenols also play a significant role as a stabilizing agent, preventing agglomeration of reduced graphene oxide nanosheets. Cytotoxicity tests showed that the both graphene oxide and *Citrullus colocynthis* polyphenol-stabilized reduced graphene oxide were toxic to DU145 cells; the cytotoxicity was dose dependent. Hence, *C. colocynthis*–mediated reduced graphene oxide may be an ideal anticancer material for biological study applications.

Keywords

Citrullus colocynthis, cytotoxicity, oxidized polyphenols, RGO

Date received: 2 June 2016; accepted: 26 February 2017

Topic: Special Issue - Graphene
Guest Editor: Yoshitaka Fujimoto

Introduction

Graphene is a novel two-dimensional nanomaterial that has attracted much attention due to its outstanding physical, chemical, and electronic properties.[1] As such, reduced graphene oxide (RGO) and its composites have been applied across a range of scientific and technical fields, such as in polymer composites, sensors, solar cells, field-effect transistors, and pharmaceutical applications.[2–8]

A number of investigations have attempted synthesis of RGO sheets using methods such as chemical vapor deposition,[9] chemical reduction of graphene oxide (GO),[10–12] and micromechanical cleavage. Among them, GO reduction by chemical methods is considered to have the greatest potential due to its low cost for industrial-scale synthesis. Additionally, graphene synthesized by chemical methods is hydrophobic and can easily aggregate due to strong π–π stacking and van der Waals interactions that exist between formed graphene sheets (GSs).[13,14]

Hence, the avoidance of GS agglomeration is of great significance, to maintain the properties of graphene in individual sheets. Functionalization is one way to overcome graphene aggregation, using either covalent or noncovalent strategies. Recently, a new approach has been developed for preparation of GSs via a nontoxic and ecofriendly method, which involves using casein, L-ascorbic acid (AA), and glucose as functionalizing and reducing agents.[15] Similarly, some plant extracts of *Terminalia*

[1] Department of Urology, Shanghai Fengxian District Central Hospital, Shanghai, People's Republic of China
[2] Urology Institute of People Liberation Army, Southwest Hospital, The Third Military Medical University, Chongqing, People's Republic of China

Corresponding author:
Jianjun Yu, Department of Urology, Shanghai Fengxian District Central Hospital, Shanghai, People's Republic of China.
Email: zhouzhansong@outlook.com

Creative Commons CC BY: This article is distributed under the terms of the Creative Commons Attribution 3.0 License (http://www.creativecommons.org/licenses/by/3.0/) which permits any use, reproduction and distribution of the work without further permission provided the original work is attributed as specified on the SAGE and Open Access pages (https://us.sagepub.com/en-us/nam/open-access-at-sage).

chebula,[16] *Terminalia bellirica*,[17] and pomegranate,[18] have also been used for synthesis of functionalized GSs. Various plant extracts and reducing sugars have already been reported for synthesis of different nanomaterials[22,19–21]; On the other hand, few electrochemical methods are reported for the green synthesis of graphene from GO.[22–25] However, the discovery of new bifunctional reagents for fast, simple, and eco-friendly synthesis of water-soluble GSs remains an ongoing challenge.

Plant extracts contain different polyphenols, such as gallic acid and tannic acid, which play a key role as reducing and capping agents during the preparation of gold and silver nanoparticles. These polyphenols may act as reducing agents during the reduction of GO and would be converted to their quinone forms.[16,17] The resulting oxidized extract polyphenols will functionalize the RGO sheets produced. In this work, we report an eco-friendly approach for the preparation of RGO using *Citrullus colocynthis* leaf extract as a reducing and stabilizing agent. The naturally available polyphenols in *C. colocynthis* leaf extract are mainly responsible for the reduction and functionalization of RGO.

Experimental section

Materials

Sodium nitrate, graphite powder (99.9995%, 100 mesh), potassium permanganate, sulfuric acid (98%), hydrogen peroxide (30%), and all other solvents were purchased from Sigma-Aldrich Chemicals Ltd (St Louis, Missouri, USA).

Preparation of C. colocynthis leaf extract

C. colocynthis leaves were separated, washed thoroughly with double distilled water, and then dried. A 1.5-g sample of dried *C. colocynthis* leaf powder was added to 100 mL of distilled water in a beaker and kept in a water bath at 70°C for 40 min. The subsequent mixture was cooled and passed through a cellulose nitrate membrane (0.2 μm) filter paper to obtain a clear extract solution.

Preparation of RGO

GO, the starting material for the synthesis of RGO, was prepared from graphite powder by following a modified Hummers method.[26] About 50 mL of *C. colocynthis* leaf extract was mixed with 50 mL of GO (1 mg mL^{-1}) and shaken thoroughly. The resulting mixture was maintained at a basic pH using NH_4OH. The subsequent reaction solution was refluxed at 100°C in a water bath for 14 h. A change in the color of the solution from brown to black indicated successful deoxygenation of GO. The formation of an RGO precipitate in the bottom of the round bottomed flask corresponds to the loss of oxygen functionalities of GO after 12 h of extract treatment.

Cytotoxicity evaluation

An in vitro cytotoxicity investigation for the prepared GO and RGO was conducted with human prostate cancer (D145) cell lines, to study viability and cellular fate. The toxicity and cell viability of DU145 cell lines were measured by exposure to a range of GO and graphene concentrations. DU145 cell lines were initially exposed to increasing GO and RGO concentrations (4, 8, 40, and 80 mg mL^{-1}). The cell viability percentage was calculated after an incubation period of 48 h using an automated cell counter. A control experiment was performed without exposure to the product; the corresponding cell growth measured was considered to be 100% viable.

Characterization

Fourier transform infrared (FTIR) analysis was performed over the 4000–500 cm^{-1} range using a JASCO FTIR 4100 spectroscopy instrument (JASCO, Japan). Samples for FTIR analysis were prepared by preparing a pellet of products with potassium bromide powder. X-ray diffraction (XRD) analysis was carried out using an Advance diffractometer (Bruker D8, Korea) over the instrumental 2θ range of 3–80°, with a step size of 0.02° using copper K_α (λ = 1.54 Å) radiation and a scan speed of 4° min^{-1}. The instrument was operated at 40 kV and 40 mA. Field emission scanning electron microscopy (FE-SEM) was performed using a JSM-7001F instrument (JSM, Japan). A JEM-2100 microscopic instrument was used for transmission electron microscopy (TEM) analysis (JEOL, USA). A dilute dispersion of RGO in water was used for TEM analysis. Thermogravimetric measurements were conducted using a Perkin-Elmer TGA-2 thermogravimetric analyzer under nitrogen at 10°C min^{-1} from room temperature to 800°C (Perkin-Elmer, Phoenix, USA). A J-Y T64000 Raman spectrometer was used for Raman measurements using an incident laser wavelength of 514.5 nm (Jobin Yivor, Japan). The thickness and surface morphology of the RGO sheets were studied using atomic force microscopy (AFM; NT-MDT Solver P47-PRO, France). A PHI Quantera scanning X-ray microprobe (SXM; ULVac-PHI Inc., Japan) was used to obtain the C1s XPS spectrum for the prepared RGO sample. Samples for X-ray photoelectron spectroscopy (XPS) measurements were prepared by uniformly coating the graphene powder on a silicon wafer surface. The high performance liquid chromatography (HPLC) chromatogram for the *C. colocynthis* extract was obtained using a Shimadzu HPLC system equipped with a diode array detector. Approximately 5 μL of *Citrullus colocynthis* extract sample was injected into the valve of the HPLC system using a Terumo Syringe (5 cc mL^{-1}) and a 25-mm Puradisc (sterile and endotoxin-free 0.2-μm Polyether sulfone syringe (PES) filter medium) at room temperature. A Hypersil Gold reverse phase (RP-18; Thermo Scientific, Waltham, Massachusetts, USA) column (250 × 4.6 mm^2; Merck, Kenilworth, New Jersey, USA) packed

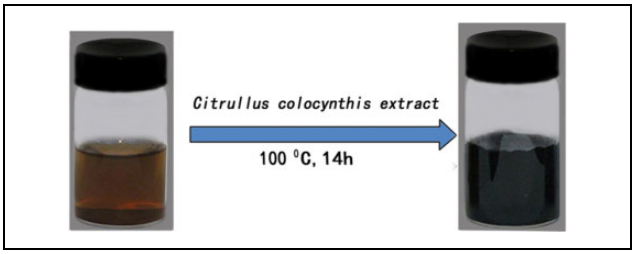


Figure 1. Schematic illustration of *Citrullus colocynthis* leaf extract induced reduction of graphene oxide.

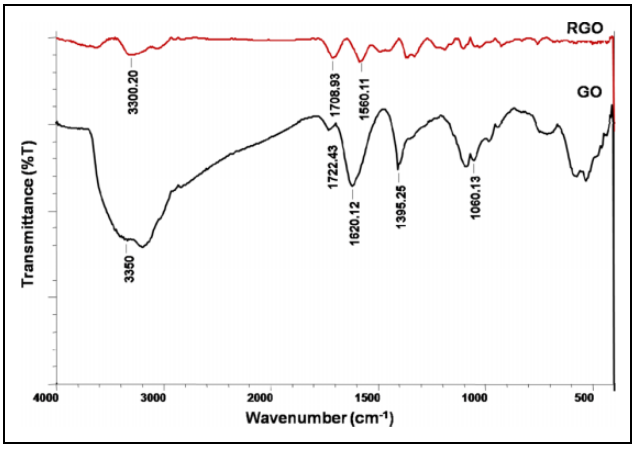


Figure 2. FTIR spectra of GO (black) and dried RGO (red). FTIR: Fourier transform infrared; RGO: reduced graphene oxide; GO: graphene oxide.

with a C18 stationary phase with a particle size of 5 µm was used for the separation of phenolic compounds. The gradient was maintained with a run rate of 1 mL min^{-1} over 10 min. The mobile phase contained a mixture of acetonitrile and water–acetic acid (99:1 v/v). Gradient elution from the column was performed with acetonitrile (13%) for approximately 10 min. The presence of flavonoids and polyphenols was detected using an ultraviolet detector at 200–500 nm. The peaks in the chromatogram were identified by comparing the retention times of reference compounds with those of analytes present in the extract.

Results and discussion

The synthetic procedure implicated in the reduction of GO is shown in Figure 1. The color change of the reaction solution from brown to black shows reduction of the GO by *C. colocynthis* extract. After completion of the reaction, the formed RGO sheets settled at the bottom of the reaction vessel as black precipitate, signifying the removal of GO functionalities containing oxygen moieties.

FTIR study

Figure 2 shows the FTIR spectra of GO and graphene. The GO spectra showed the presence of a rich collection of

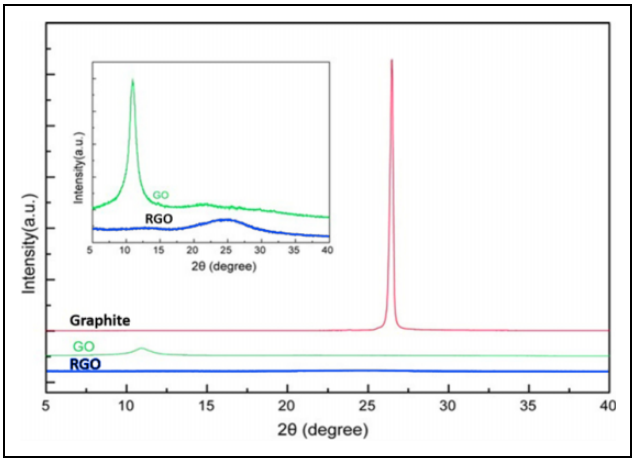


Figure 3. XRD patterns of GO (green) and RGO (blue) and graphite (pink). RGO: reduced graphene oxide; GO: graphene oxide; XRD: X-ray diffraction.

vibrational bands characteristic of O–H at 3400 and 1395 cm^{-1} (O–H stretching), Ketone group at 1720 cm^{-1} (C=O stretching), C=C at 1620 cm^{-1} (C=C stretching), and C–O at 1060 cm^{-1} (C–O stretching). The FTIR spectrum of RGO is represented by the peaks at 1550 and 1190 cm^{-1} corresponding to C=C conjugation and C–C band stretching vibrations. The absence of peaks corresponding to oxygen functionalities in the RGO spectrum further confirms the loss of oxygen containing functional groups after reduction of GO.[16]

XRD study

Figure 3 shows the XRD patterns of graphite powder, GO, and RGO. The XRD pattern of the graphite powder showed the presence of a sharp diffraction peak at 2θ of 26.5°, signifying the high crystallinity of the graphite powder used. The presence of a new peak at 2θ of 11.3° is observed upon oxidation, which indicates the formation of GO. Concurrently, the interlayer spacing of GO is increased after oxidation from 0.336 nm (d-spacing of graphite) to 0.77 nm, due to the generation of O-containing functionalities and water molecules. After the reduction of GO, the GO diffraction peaks disappeared and a new weak graphene peak was observed at $2\theta = 26.0°$, indicating that the RGO sheets obtained existed individually with a highly disordered nature.[17]

FE-SEM and TEM analyses

Figure 4(a) shows the FE-SEM image of RGO sheets, in which graphene nanosheets emerge as wave-shaped corrugated structures, forming a disordered RGO solid. The TEM image shown in Figure 4(b) confirms the presence of individual GSs. The TEM image also shows the thin, transparent nature of the GSs, resembling a crumpled fabric with folded edges.[27]

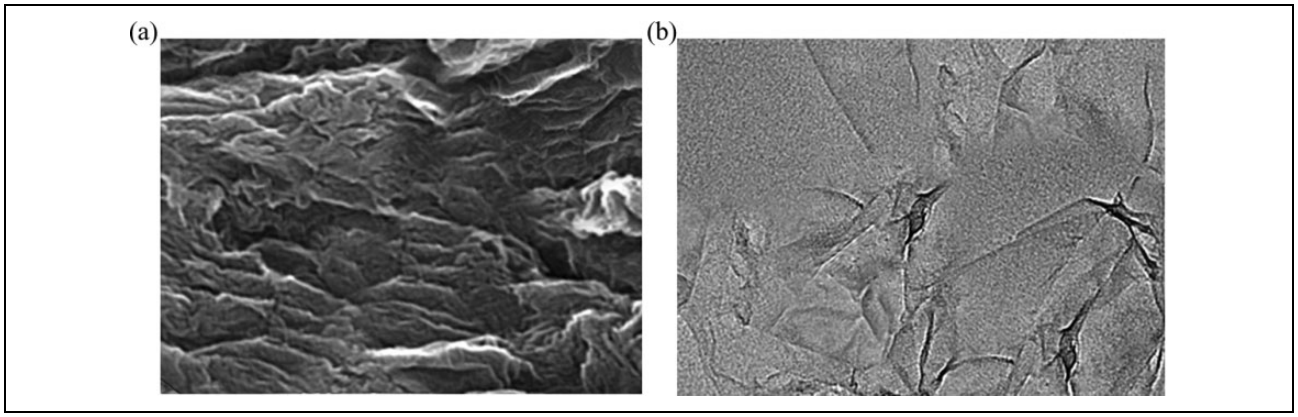


Figure 4. FE-SEM image (a) and TEM image (b) of *Citrullus colocynthis* leaf extract mediated RGO. RGO: reduced graphene oxide; FE-SEM: field emission scanning electron microscopy.

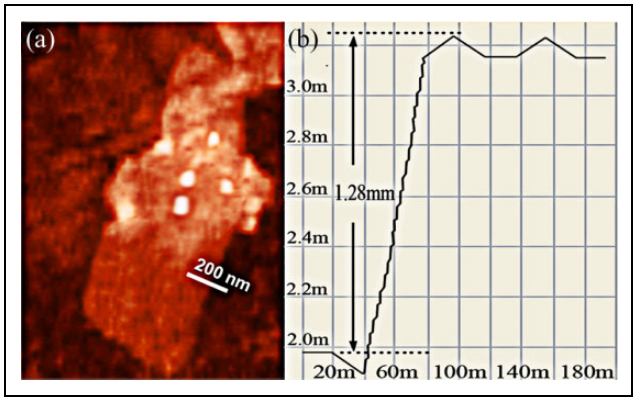


Figure 5. AFM image (a) and height profile (b) of RGO sheets. RGO: reduced graphene oxide; AFM: atomic force microscopy.

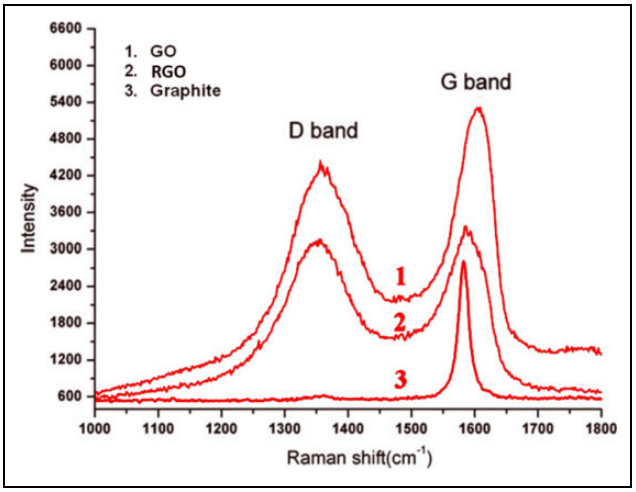


Figure 6. Raman spectra of GO (1), RGO (2), and graphite (3). RGO: reduced graphene oxide; GO: graphene oxide

AFM analysis

The GS thickness was obtained using AFM. For thickness measurements, the RGO sample was initially coated on the surface of a mica sheet by spin coating. Figure 5(a) shows the AFM image of the aqueous graphene dispersion; the synthesized GSs are well separated in the graphene dispersion solution. Similarly, the thickness of the RGO sheets, obtained from the height profile of the GSs (shown in Figure 5(b)), was 1.28 nm, larger than that reported for a single-layer GS (approximately 1 nm).[28] Although most of the oxygen functionalities are removed after reduction, it is reasonable to conclude that plant extract polyphenols may play a key role in increasing the thickness of the synthesized GSs.[29] These polyphenols that are adsorbed on graphene surface, further prevent their agglomeration by creating electrostatic repulsions between the GSs. Also, these polyphenols increase the aqueous dispersibility of graphene without adding any external reagents or surfactants.

Raman analysis

Raman spectroscopy is a powerful technique widely used to study structural changes, such as disorder and defects in graphene materials. The G band is associated with the sp^2-bonded in-plane vibration of carbon atoms. Similarly, the D band represents the sp^3 vibrations of C-atoms of disordered graphene. In contrast, the I_D/I_G ratio of synthesized RGO (shown in Figure 6) was higher than that of GO, indicating a significant reduction in sp^3-carbon content as well as other oxidized molecular defects.[16]

XPS study

C1s XPS spectra for both GO and RGO were examined in an attempt to better understand the reduction of GO. The high-resolution C1s XPS spectrum of synthesized GO and RGO is shown in Figure 7. The C1s spectrum of both GO and RGO showed peaks at 284.5, 286.2, and 286.8 eV corresponding to the C–C, C–O, and C=O groups respectively. However, the relatively reduced C–O peak intensity in the C1s spectrum of RGO, compared with that of GO, further indicated the successful loss of oxygen functionalities after GO reduction.

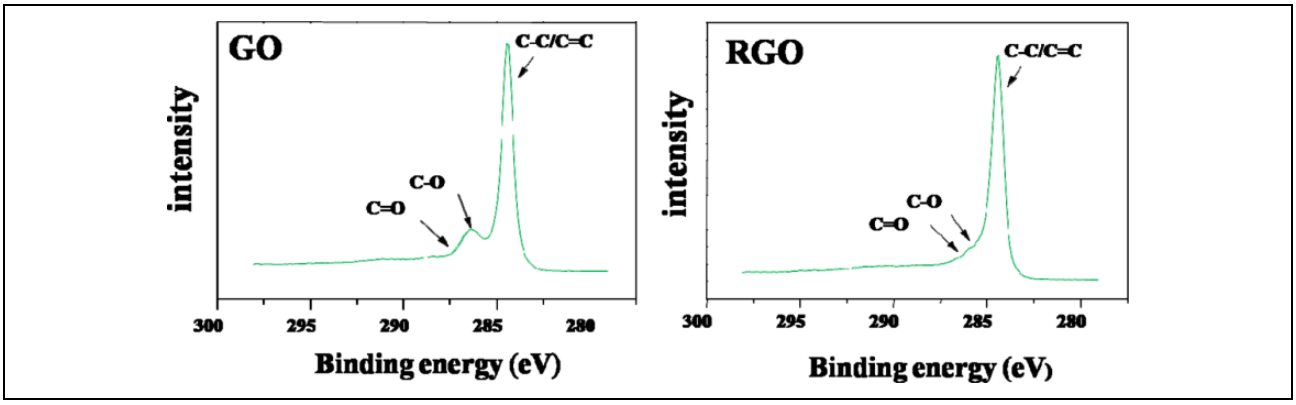


Figure 7. C1s XPS spectrum of GO and RGO prepared by using *Citrullus colocynthis* leaf extract. RGO: reduced graphene oxide; GO: graphene oxide; XPS: X-ray photoelectron spectroscopy.

Table 1. Polyphenols and flavonoids of *Citrullus colocynthis* leaf extract.

S. No	Bioconstituents of *Cinnamomum tsoi* extract	Area (%)
1	Gallic acid	1.96 ± 0.59
2	4-Hydroxycinnamic acid	0.50 ± 0.56
3	4-Hydroxy-3-methoxycinnamic acid	1.11 ± 0.31
4	Vanillic acid	2.41 ± 0.52
5	Apigenin	0.36 ± 0.81
6	Kaempferol	3.32 ± 0.67
7	Luteolin	1.39 ± 0.80
8	Naringenin	1.38 ± 0.23
9	Quercetin	65.66 ± 0.12

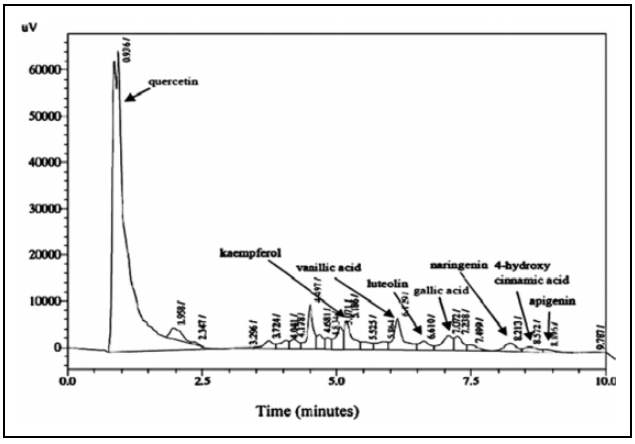


Figure 8. HPLC chromatogram of aqueous *Citrullus colocynthis* leaf extract. HPLC: high performance liquid chromatography.

Mechanism

Phytochemical analyses of plant leaves reported in the literature identified the presence of polyphenols in aqueous extracts. For instance, Maddinedi et al. reported the existence of polyphenols such as gallic acid, pyrogallol, AA, and methyl gallate in the aqueous extract of *T. chebula*.[16] Similarly, an aqueous extract of *T. bellirica* showed the presence of gallic acid, pyrogallol, AA, resorcinol, and methyl gallate.[17] HPLC studies performed on *C. colocynthis* also showed the presence of various flavonoids and polyphenols such as luteolin, gallic acid, naringenin, 4-hydroxycinnamic acid, kaempferol, 4-hydroxy-3-methoxycinnamic acid, apigenin, vanillic acid, and quercetin in aqueous extract (Table 1, Figure 8). Quercetin was found at the highest rate of approximately 65.66 ± 0.12%; other biomolecules were found at lower levels as follows: luteolin (1.39 ± 0.80%), kaempferol (3.32 ± 0.67%), apigenin (0.36 ± 0.81%), and naringenin (1.38 ± 0.23%). In contrast, the HPLC chromatogram showed that vanillic acid (2.41 ± 0.52%) and gallic acid (1.96 ± 0.5%) were present at higher levels than the other polyphenols. These bioconstituents are involved in deoxygenation and subsequent decoration of the RGO surface. The –OH groups of polyphenols present in plant extracts will undergo SN_2 nucleophilic substitution with the –OH groups present in GO, resulting in the reduction of GO via the elimination of two water molecules. The generated oxidized polyphenols will then stabilize the formed RGO sheets via π–π stacking interactions.

The decoration of RGO by oxidized polyphenols was further supported by the negative surface charge of the RGO sheets obtained, which was found to be −14.4 mV (shown in Figure 9.). On the other hand, the surface charge of GO is found to be −33 mV. However, the negative zeta potential of the GSs may be due to oxygen-containing groups present in oxidized polyphenols that exist on the surface of RGO after reduction. These oxidized polyphenols lead to increased stability of GSs by preventing agglomeration. In contrast, GSs prepared using chemicals, such as sodium borohydride, phenylhydrazine, and hydrazine, were not stable due to the lack of capping molecules on their surface, preventing agglomeration. The graphene prepared using *C. colocynthis* extract was highly stable, and biomolecules on the formed graphene surface increased stability by preventing aggregation. This attribute has the potential to advance applications in science and technology fields, as the majority of the properties of RGO are associated with individual GS. Additionally, the RGO prepared using the plant extract was

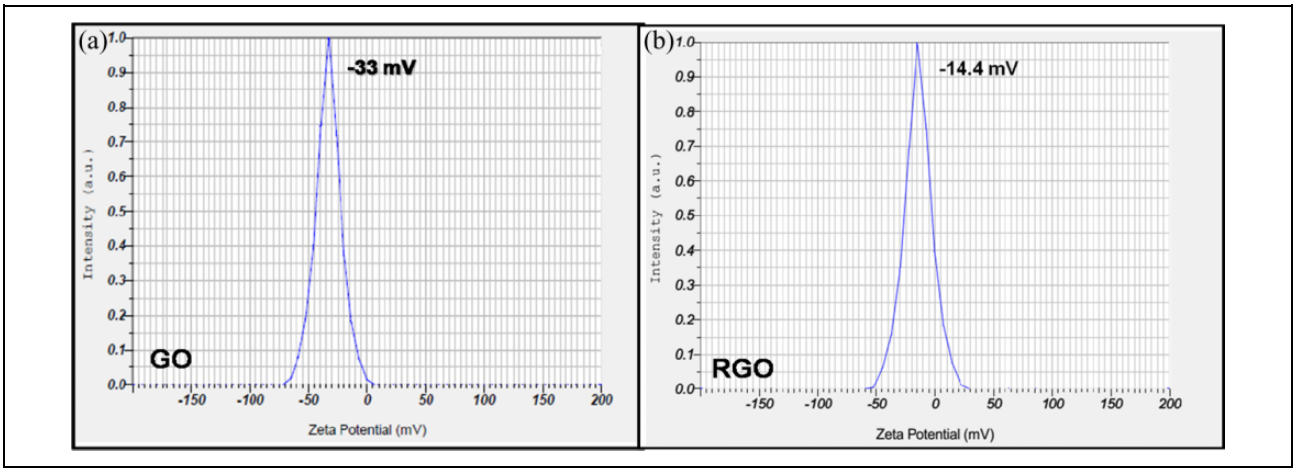


Figure 9. Zeta potential of GO (a) and RGO synthesized by using *Citrullus colocynthis* leaf extract (b). RGO: reduced graphene oxide; GO: graphene oxide.

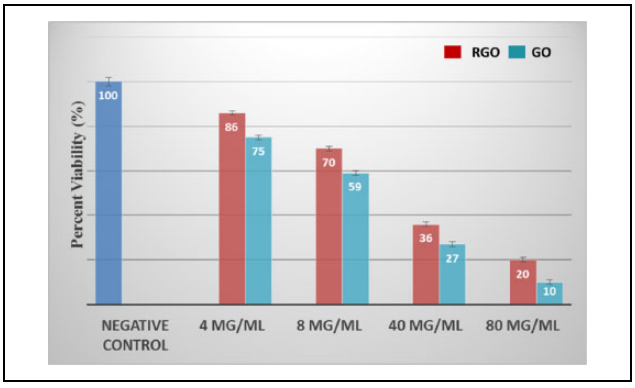


Figure 10. Cell viability of DU145 cell lines induced by GO and RGO. RGO: reduced graphene oxide; GO: graphene oxide.

dispersible in water. These characteristics explain the most significant advantages of RGO prepared using plant extracts in biomedical applications.[17]

In vitro cytotoxicity

GSs were effectively prepared to examine their in vitro cytotoxicity using DU145 cell lines in water medium. The toxic effect of RGO concentration on the cell viability percentage of DU145 cell lines was studied by exposing them to various concentrations of GO and RGO (4, 8, 40, and 80 mg mL^{-1}). The cytotoxicity studies showed that both GO and RGO were toxic toward DU145 cell lines. It can be seen from Figure 10 that the percentage cell viabilities were 75% and 10% for GO and 86% and 20% for RGO, when exposed to concentrations of 4 and 80 mg mL^{-1}, respectively.

It is notable that the cytotoxicities of GO and RGO increased with exposure concentration. In addition, GO was found to be more toxic to DU145 cell lines than RGO. It is likely that the cytotoxicity of graphene-based materials mainly depends on the physicochemical features of the material, such as the conductivity, size, and density of the functional groups as well as the type of deoxygenating agent used for GO reduction, the degree of functionalization, and the cell type used for the study.[30] The main advantage of using graphene materials for cytotoxicity includes their biocompatibility toward cancer cells when compared to other nanomaterials. The toxicity of carbon nanomaterials is heavily influenced by their functionalization degree. GO contains many oxygen atoms in the forms of carboxyl groups, epoxy groups and hydroxyl groups. According to the oxygen content, the functionalization degree of GO is generally higher than that of other nanomaterials such as carbon nanotubes and metal nanoparticles.[31] Therefore, the good biocompatibility of GO is generally expected to this regard. Further, the biocompatibility of graphene materials increases their scope of applications in drug delivery and biomedicine.

The dose-dependent toxicity of other nanomaterials, such as gold nanoparticles, against HCT116, A549 cell lines has been reported.[32] From these results, it can be concluded that the cytotoxicity of green-synthesized RGO is dose dependent. Thus, the GSs synthesized using *C. colocynthis* extract could potentially act as an anticancer agent, which may be used for the development of new anticancer drugs. Further, the confirmation of the effect by a cytotoxicity screening assay and comparison to the action on normal cells is needed to identify the mechanism of cytotoxicity of GO and RGO toward cancer cells, which will be studied in our future work.

Conclusions

In this work, we showed a facile, low-cost, green preparation method for the deoxygenation of GO using *C. colocynthis* leaf extract polyphenols. Raman, XRD, and XPS data showed the effective deoxygenation of GO. Cytotoxicity results showed that the synthesized RGO acts as an effective anticancer agent and that the cytotoxicity is dose dependent. This synthetic approach showed the industrial production of RGO in an eco-friendly way using plant extracts.

Acknowledgments

The authors are thankful to Shanghai Fengxian District Central Hospital and the Third Military Medical University for providing fund and platform to do this research.

Declaration of conflicting interests

The author(s) declared no potential conflicts of interest with respect to the research, authorship, and/or publication of this article.

Funding

The author(s) disclosed receipt of the following financial support for the research, authorship, and/or publication of this article: This work was financially supported by Shanghai Fengxian District Central Hospital and the Third Military Medical University.

References

1. Akhavan O, Ghaderi E and Rahighi R. Toward single-DNA electrochemical biosensing by graphene nanowalls. *Nature* 2012; 6: 2904–2916.
2. Geim AK and Novoselov KS. The rise of graphene. *Nature Mater* 2007; 6: 183–191.
3. He Q, Sudibya HG, Yin Z, et al. Micropatterns of reduced graphene oxide films. *Fabrication and Sensing Applications* 2010; 4: 3201–3208.
4. Wang Z, Zhang J, Chen P, et al. Label-free, electrochemical detection of methicillin-resistant staphylococcus aureus DNA with reduced graphene oxide-modified electrodes. *Biosens Bioelectron* 2011; 26: 3881–3886.
5. Stankovich S, Dikin DA, Dommett GHB, et al. Graphene-based composite materials. *Nature* 2006; 442: 282–286.
6. Yin Z, Sun S, Salim T, et al. Organic photovoltaic devices using highly flexible reduced graphene oxide films as transparent electrodes. *ACS Nano* 2010; 4: 5263–5268.
7. Dreyer DR, Park S, Bielawski CW, et al. The chemistry of graphene oxide. *Chem Soc Rev* 2010; 39: 228–240.
8. Yin Z, Wu S, Zhou X, et al. Electrochemical deposition of ZnO nanorods on transparent reduced graphene oxide electrodes for hybrid solar cells. *Small* 2010; 6: 307–312.
9. Eizenberg M and Blakely JM. Carbon monolayer phase condensation on Ni(111). *Surf Sci* 1979; 82: 228–236.
10. Bagri A, Mattevi C, Acik M, et al. Structural evolution during the reduction of chemically derived graphene oxide. *Nat Chem* 2010; 2: 581–587.
11. Park S and Ruoff RS: Chemical methods for the production of graphenes. *Nat Nanotechnol* 2009; 4: 217–224.
12. Stankovich S, Dikin DA, Piner RD, et al. Synthesis of graphene-based nanosheets via chemical reduction of exfoliated graphite oxide. *Carbon* 2007; 45: 1558–1565.
13. Wang G, Yang J, Park J, et al. Facile synthesis and characterization of graphene nanosheets. *J Phys Chem C* 2008; 112: 8192–8195.
14. Si Y, Samulski ET, Hill C, et al. Synthesis of water soluble graphene. *Nano Lett*. 2008; 8: 1679–1682.
15. Paredes JI, Villar-Rodil S, Fernandez-Merino MJ, et al. Environmentally friendly approaches toward the mass production of processable graphene from graphite oxide. *J Mater Chem* 2011; 21: 298–306.
16. Maddinedi SB, Mandal BK, Vankayala R, et al. Bioinspired reduced graphene oxide nanosheets using Terminalia chebula seeds extract. *Spectrochim Acta A Mol Biomol Spectrosc* 2015; 145: 117–124.
17. Maddinedi SB and Mandal BK. Biofabrication of reduced graphene oxide nanosheets using terminalia bellirica fruit extract. *Current Nanosci* 2015; 12: 94–102.
18. Farnosh T, Masoud SN, Alireza B, et al. Green synthesis and characterization of graphene nanosheets. *Mater Res Bulle* 2015; 63: 51–57.
19. Farnosh T, Masoud SN and Fatemeh M. Green synthesis of flower-like CuI microstructures composed of trigonal nanostructures using pomegranate juice. *Mater Lett* 2013; 100: 133–136.
20. Farnosh T, Masoud SN, Davood G, et al. Application of glucose as a green capping agent and reductant to fabricate CuI micro/nanostructures. *Mater Res Bulle* 2014; 49: 14–20.
21. Samira M, Faezeh S and Masoud SN. Sol–gel auto combustion synthesis of BaFe12O19nanoceramics by using carbohydrate sugars as a novel reducing agent. *Adv Powder Technol* 2015; 26: 1348–1354.
22. Kakaei K. One-pot electrochemical synthesis of graphene by the exfoliation of graphite powder in sodium dodecyl sulfate and its decoration with platinum nanoparticles for methanol oxidation. *Carbon* 2013; 51: 195–201.
23. Kakaei K and Hasanpour K. Synthesis of graphene oxide nanosheets by electrochemical exfoliation of graphite in cetyltrimethylammonium bromide and its application for oxygen reduction. *J Mater Chem A* 2014; 2: 15428–15436.
24. Kakaei K. Decoration of graphene oxide with Platinum Tin nanoparticles for ethanol oxidation Electrochim. *Acta* 2015; 165: 330–337.
25. Kakaei K and Dorraji M. One-pot synthesis of Palladium Silver nanoparticles decorated reduced graphene oxide and their application for ethanol oxidation in alkaline media. *Electrochim. Acta*. 2014; 143: 207–215.
26. Perera SD, Mariano RG, Nijem N, et al. Alkaline deoxygenated graphene oxide for supercapacitor applications: an effective green alternative for chemically reduced graphene. *J Power Sources* 2012; 215: 1–10.
27. Chang HX, Wang GF, Yang A, et al. A transparent, flexible, low-temperature, and solution-processible graphene composite electrode. *Adv Funct Mater* 2010; 20: 2893–2902.
28. Li D, Müller MB, Gilje S, et al. Processable aqueous dispersions of graphene nanosheets. *Nat Nanotechnol* 2008; 3:101–105.
29. Su Q, Pang SP, Alijani V, et al. Composites of graphene with large aromatic molecules. *Adv Mater* 2009; 21: 3191–3195.
30. Gurunathan S, Han JW, Kim E, et al. Enhanced green fluorescent protein-mediated synthesis of biocompatible graphene. *J Nanobiotechnology* 2014; 12: 41.
31. Chang Y, Yang ST, Liu JH, et al. In vitro toxicity evaluation of graphene oxide on A549 cells. *Toxicology Lett* 2011; 200: 201–210.
32. Maddinedi SB, Mandal BK, Ranjan S, et al. Diastase assisted green synthesis of sizecontrollable gold nanoparticles. *RSC Adv* 2015; 5: 26727–26733.